

## General Disclaimer

### One or more of the Following Statements may affect this Document

- This document has been reproduced from the best copy furnished by the organizational source. It is being released in the interest of making available as much information as possible.
- This document may contain data, which exceeds the sheet parameters. It was furnished in this condition by the organizational source and is the best copy available.
- This document may contain tone-on-tone or color graphs, charts and/or pictures, which have been reproduced in black and white.
- This document is paginated as submitted by the original source.
- Portions of this document are not fully legible due to the historical nature of some of the material. However, it is the best reproduction available from the original submission.

DRA

(NASA-CR-175371) EFFECTS OF SYSTEMATIC  
ERRORS ON THE MIXING RATIOS OF TRACE GASES  
OBTAINED FROM OCCULTATION SPECTRA (Jet  
Propulsion Lab.) 35 p HC A03/MF A01

N84-18046

Unclas  
CSCL 20F G3/74 00573

**Effects of Systematic Errors on the Mixing Ratios of  
Trace Gases Obtained from Occultation Spectra \***

W. A. Shaffer and J. H. Shaw

Department of Physics

The Ohio State University

Columbus, OH 43210

and

C. B. Farmer

Jet Propulsion Laboratory

Pasadena, CA 91103



\* This work was supported in part by NASA Grant NSG-7469.

## Abstract

The influence of systematic errors in the parameters of the models describing the geometry and the atmosphere on the profiles of trace gases retrieved from simulated solar occultation spectra, collected at satellite altitudes, is investigated. It is concluded that, because of smearing effects and other uncertainties, it may be preferable to calibrate the spectra internally by measuring absorption lines of an atmospheric gas such as CO<sub>2</sub> whose vertical distribution can be assumed rather than to rely on externally supplied information.

## Introduction

It is expected that high-resolution, infrared, solar, occultation spectra covering wide spectral regions will soon be collected from satellite altitudes.<sup>1</sup> These spectra will add significantly to our knowledge of atmospheric properties, including the latitudinal and vertical distributions of many trace gases. However, the quantitative analysis of these spectra requires a knowledge of the geometry of the experiment and of the characteristics of the atmosphere along the ray paths. Although this information can be obtained from external sources, features in the collected spectra, including, for example, those of gases such as CO<sub>2</sub>, whose vertical mixing-ratio profiles are well known, can be used to calibrate the spectra internally.<sup>2</sup>

In this paper the influence of systematic errors in the path geometry and the atmospheric characteristics on the derived mixing-ratio profiles of trace gases is estimated with the simulation methods used previously.<sup>2</sup> It is assumed that the data consist of the equivalent widths of weak lines. The relative merits of internal and external calibration of spectra obtained from satellite altitudes are compared and it is concluded that, in many cases, it may be preferable to calibrate the spectra internally by measuring lines of a gas such as CO<sub>2</sub> whose vertical and latitudinal distribution is reasonably constant.<sup>4</sup> Farmer et al.<sup>2</sup> have previously found that calibrations, based on CO<sub>2</sub> lines, of solar spectra obtained from balloon altitudes also reduced systematic errors associated with the atmospheric models and observational geometry.

Systematic Errors Associated with the External Calibration Method.

The equivalent width of a weak atmospheric line can be written as

$$W(z_i) = \sum_j S_j \rho_j d_j \delta l_{ij} \quad (1)$$

where  $S_j$  is the line intensity,  $\rho_j$  is the mixing-ratio of the absorbing gas,  $d_j$  is the air density, and  $\delta l_{ij}$  is the path length in the  $j$ th atmospheric layer traversed by the  $i$ th ray which reaches the instrument at an angle  $z_i$  with respect to the local zenith. Some of the quantities affecting these equivalent widths are summarized in Table 1. In general, if the line intensity depends on parameters  $s$ , the mixing ratio on parameters  $t$ , the density on parameters  $x$ , and the incremental path on parameters  $y$ , then the change in equivalent width caused by changes in these parameters

$$dW(z_i) = \sum_j S_j \rho_j d_j \delta l_{ij} \left[ \frac{1}{S_j} \sum_g \frac{\partial S_j}{\partial s_g} \Delta s_g + \frac{1}{\rho_j} \sum_p \frac{\partial \rho_j}{\partial t_p} \Delta t_p + \frac{1}{d_j} \sum_q \frac{\partial d_j}{\partial x_q} \Delta x_q + \frac{1}{\delta l_{ij}} \sum_r \frac{\partial \delta l_{ij}}{\partial y_r} \Delta y_r \right] \quad (2)$$

It is convenient to assume, initially, that the line intensity is known accurately and is independent of temperature. In this case the amount of absorber  $a(z_i)$  along the incoming rays

$$a(z_i) = W(z_i) / S \quad (3)$$

and

$$\Delta a(z_i) = \sum_j \rho_j d_j \delta l_{ij} \left[ \frac{1}{\rho_j} \sum_p \frac{\partial \rho_j}{\partial t_p} \Delta t_p + \frac{1}{d_j} \sum_q \frac{\partial d_j}{\partial x_q} \Delta x_q + \frac{1}{\delta l_{ij}} \sum_r \frac{\partial \delta l_{ij}}{\partial y_r} \Delta y_r \right] \quad (4)$$

where we have assumed that the set of  $x$  variables is independent of the set of  $y$  variables and the set of  $t$  variables is the union of the  $x$  and  $y$  sets.

The effects of errors in  $d_j$  and  $\delta l_{ij}$  on the values of  $\rho_j$  retrieved from a set of  $a(z_i)$  values have been studied by creating a set of measurements  $a(z_i)$  with an appropriate

ORIGINAL PAGE IS  
OF POOR QUALITY

set of values for the parameters  $x_q$  and  $y_r$ . Mixing ratio profiles were retrieved successively from these data using incorrect values for each of the parameters  $x_q$  or  $y_r$ . If, for example, the incorrect value  $x_1 + \Delta x_1$  was used then, since the correct set of absorber amount values were analyzed,  $\Delta a(x_1) = 0$ , and Eq. (4) becomes

$$\sum_j \left[ \frac{1}{\rho_j} \frac{\partial \rho_j}{\partial x_1} \Delta x_1 + \frac{1}{d_j} \frac{\partial d_j}{\partial x_1} \Delta x_1 \right] = 0.$$

This can be written as

$$\sum_j \frac{\Delta \rho_j}{\rho_j} + \frac{\Delta d_j}{d_j} = 0.$$

If the local mixing-ratio values are independent then

$$\frac{\Delta \rho_j}{\rho_j} + \frac{\Delta d_j}{d_j} = 0,$$

similarly

$$\frac{\Delta \rho_j}{\rho_j} + \frac{\Delta \delta_{ij}}{\delta_{ij}} = 0.$$

(5)

The program described by Snider and Goldman<sup>5,6</sup> was used to calculate the absorber amounts along the paths of 125 rays, with nearly equally-spaced tangent heights between 0 and 50 km, to a satellite 500 km above the surface and at 45° latitude. The absorber was assumed to have a constant mixing-ratio in all three dimensions and to be in an atmosphere with the temperature and density profile of the U.S. Standard Atmosphere.<sup>7</sup> A wavelength of 5  $\mu$ m was assumed.

For these conditions the distance along a ray, such as that shown in Fig. 1, from the tangent point to the satellite is about 2500 km and the distance to a point 50 km above the tangent point is about 800 km. Variations in the effective radius of the earth or in the atmospheric temperature, density, and mixing-ratio profiles along these paths have

not been modelled, nor have the effects of the finite FOV of the instrument and satellite motion during the period of data collection. Kantor<sup>8</sup> has shown the variability of the density of the atmosphere between 20 and 60 km above the surface from the equator to 65° over periods of up to 72 hours and distances of up to 370 km is typically several percent. The finite angular FOV causes a spread of the beam at the tangent point of about 2.5 km/mrad. Satellite motion may cause the tangent heights of the rays to change at rates as high as 3 km/sec. Thus the vertical resolution of typical measurements made with a FOV of 1 mrad and for observation times of about one second is limited to a few kilometers. These effects also set upper limits to the accuracy of the information which can be derived from the spectra.

#### Layer Thickness

The paths of rays through the atmosphere and the total air mass traversed were calculated by dividing the atmosphere into layers with the same vertical thickness. The dependence of these calculated air masses on layer thickness is shown in Fig. 2 for thicknesses of from 25 m to 20 km and rays with tangent heights of 2.6, 12, and 48 km. The calculations are made by assuming there is a constant vertical temperature gradient in each layer. For the two lowest rays, this is a good approximation for all layer thicknesses. The larger variations in the calculated air mass traversed by the ray with a tangent height of 48 km are attributed to the rapid changes in the temperature gradient of the Standard Atmosphere near 50 km. In the rest of this work a layer thickness of 0.25 km was used. This still caused irregularities seen in some of the figures near the tropopause level.

### Atmospheric Refraction

The atmospheric dispersion from the visible to beyond 20  $\mu\text{m}$  is small and, to a very good approximation, rays of all wavelengths can be assumed to travel the same paths. However, if refraction is not considered, the calculated air masses traversed by rays with tangent heights between 0 and 90 km have the errors shown in Fig. 3. If the mixing ratio profile is retrieved by neglecting refraction, the calculated path segments  $\delta l_{ij}$  required in Eqs. 1 and 5 are incorrect and errors in the retrieved mixing-ratio profiles are produced, as shown in Fig. 4. The irregularity near 10 km is due to the rapid change in the atmospheric temperature gradient at the tropopause.

### Reference Pressure Errors

The atmospheric pressure and density profiles were obtained from the vertical temperature profile and the sea level pressure  $P_0$ . If the correct temperature profile is used, the pressure and density at any other level and the air mass traversed by a ray with a fixed tangent height are proportional to  $P_0$ . Thus

$$\Delta d/d = \Delta P_0 / P_0, \quad (6)$$

and hence from Eq. (5)

$$\Delta \rho / \rho = -\Delta P_0 / P_0. \quad (7)$$

The fractional errors in the retrieved mixing-ratio,  $\Delta \rho / \rho$ , shown in Fig. 5, and obtained for the case where the ray path geometry is known accurately but  $\Delta P_0 / P_0$  is equal to  $\pm 5\%$ , are not independent of height, as expected from Eq. (7), because the change in the air density causes the refraction effects to be modelled incorrectly.



Incorrect reference level pressures may be used because of uncertainties in the large-scale, global variations in atmospheric pressure, density, and temperature. In addition, smaller-scale variations in these quantities of several percent may occur over regions much smaller than those traversed by the rays.<sup>8</sup> These variations are difficult to model in the spectral analyses described here and they may limit the accuracy of the retrieved mixing-ratio profiles. Since pressure and height are related, the use of an incorrect reference pressure at a known altitude is equivalent to choosing an incorrect altitude for the reference pressure. These relations can be estimated for an isothermal atmosphere in which the pressure and density are given by

$$P(h) = P_0 \exp(-h/H), \quad (8)$$

$$\text{and } d(h) = d_0 \exp(-h/H), \quad (9)$$

where the scale height of the atmosphere

$$H = RT/Mg, \quad (10)$$

is approximately 7 km below 50 km in the Standard Atmosphere.

Since

$$\Delta h/H = \Delta P / P_0, \quad (11)$$

a five percent error in  $P_0$  is equivalent to an error of 0.4 km in the tangent heights of all the rays.

#### Errors in Atmospheric Temperature

The dependence of atmospheric density on temperature can be approximated by considering an isothermal atmosphere with a fixed reference pressure  $P_0$ . From Eqs. (8) and (10)

$$\Delta P = MghP\Delta T/RT^2,$$

ORIGINAL PAGE IS  
OF POOR QUALITY (12)

and, for a perfect gas,

$$d = MP/RT.$$

Thus 
$$\Delta d = M\Delta P/RT - MP\Delta T/RT^2, \quad (13)$$

and 
$$\Delta d/d = (h - H)\Delta T/HT. \quad (14)$$

As the temperature of the entire atmosphere is changed the density remains constant near  $h = H$  but it increases at a rate of about 2.5%/K near 50 km. From Eq. (4) the dependence of the errors in the retrieved mixing-ratio profiles on these density changes is also described by Eq. (14).

The fractional changes in the atmospheric density caused by changing the temperatures at all levels in the standard atmosphere by  $\pm 5\%K$  and the corresponding fractional errors in the retrieved mixing-ratios in Fig. 6 are similar to those predicted by Eq. (14). Larger errors in the mixing-ratio may occur if the line intensities depend on temperature. It is planned to discuss these effects elsewhere since they may be used to obtain improved estimates of the temperature profile if the mixing-ratio of the absorbing gas is known.

The differences in the tangent heights of rays which pass through the same air masses in isothermal atmospheres at different temperatures are obtained from Eqs. (9) and (14)

$$\Delta h = (H - h)\Delta T/T. \quad (15)$$

These differences increase to about 0.4 km near 50 km for a one percent change in the temperature of the entire atmosphere. In addition to mixing-ratio errors caused by

the use of incorrect vertical temperature profiles unmodelled horizontal temperature variations may also affect the accuracy of the retrieved mixing-ratio profiles.

#### Satellite Heights

It is seen from Fig. 1 that a change  $\Delta a$  in the satellite height causes a change  $\Delta a \cos\theta \approx \Delta a$  in the tangent heights of all the rays. From Eq. (9)  $\Delta d/d + \Delta h/H = 0$ . Thus, for an isothermal atmosphere, the rate of change of density with height, and hence of the air mass traversed with the tangent height of a ray, is about 14%/km. The errors in the retrieved mixing-ratios caused by errors of  $\pm 1$  km in the satellite height, shown in Fig. 7, are approximately 14% and the vertical dependence is very similar to that caused by errors in  $P$ . To reduce the errors to less than 1% the satellite height must be known to better than 100 m.

#### Latitude Error

The effective radius of the earth and the acceleration due to gravity are both latitude dependent and the air masses traversed by rays reaching an observer at fixed incoming angles vary with latitude. A series of calculations has shown that, for an observer at 50 km, the air masses traversed by the rays varied by less than  $\pm 4\%$  from the value at  $45^\circ$ , as the latitude was varied from  $0^\circ$  to  $90^\circ$ , and the changes were essentially the same for all rays with tangent heights between 0 and 50 km. Thus, since the latitude is always well determined, these changes should not be a significant source of error.

Incoming Angle Errors

Atmosphere paths are calculated from the angle  $z$  shown in Fig. 1, between the local zenith and the arriving rays. This angle can be measured directly or it can be calculated from the known position of the instrument and the time of observation, provided atmospheric refraction is included.

An error  $\Delta z$  in this angle causes an error  $\Delta b \approx L\Delta z$  in the tangent height, where  $L$  is the satellite-to-tangent height distance. For a satellite at 500 km,  $\Delta b/\Delta z$  is approximately 2.4 km/mr or 40 km/1°. This corresponds to a rate of change in the atmospheric density at the tangent height of about 600%/1°. The changes in the retrieved mixing-ratio caused by systematic errors in  $z$  of 0.01° and corresponding errors in  $b$  of 0.4 km are shown in Fig. 8. As expected, they are nearly independent of height and average about 6%.

When the angle  $z$  is calculated from the parameters of the satellite orbit, errors may arise from incorrect estimates of the satellite height, the position in its orbit, the plane of the orbit, or the time of observation. For the two-dimensional geometry in Fig. 1

$$z = 90 + \theta, \quad (16)$$

$$\Delta z = \Delta \theta.$$

$$\cos \theta = (R + b)/(R + a), \quad (17)$$

$$\Delta b = L\Delta z,$$

and 
$$-\sin \theta \Delta \theta = -(R + b)\Delta a/(R + a)^2 + (a - b)\Delta R/(R + a)^2 + \Delta b/(R + a).$$

For a satellite with  $a = 500$  km,  $R = 6400$  km, and  $b \ll a$ , errors of 0.5 km in  $a$ , of 6 km in  $R$ , or of 0.01° in  $\theta$  or  $z$  cause 7% errors at all heights in the derived

ORIGINAL PAGE IS  
OF POOR QUALITY

mixing-ratio profile. The same error is caused if the position of the satellite in its orbit is uncertain by 1.2 km or if there is a timing error of 0.16 sec. Since all of these errors affect the derived mixing-ratio profiles in the same manner as errors in the reference pressure, additional information must be supplied if the origins of suspected errors are to be identified.

#### Satellite Motion

For the two-dimensional geometry in Fig. 1 and for a satellite in a circular orbit at 500 km the tangent height of a ray changes at a rate of about 2.8 km/sec, in the absence of refraction. The distortion of these paths due to changes in the atmospheric density gradient and to refraction have been discussed by Garriott<sup>9</sup> and Russell.<sup>10</sup>

The corresponding rate of change of air mass, in an isothermal atmosphere, obtained from Eq. 9 is about 40%/sec. These rates of change of air mass as functions of the change in apparent zenith angle were also calculated for an atmosphere with a temperature gradient of 1 K/km and for the U. S. Standard Atmosphere with refraction effects included. The results are shown in Fig. 9. In both cases the mean rate is about 40%/sec. However the rate varies significantly with the tangent heights of the rays because it is affected both by refraction and by the atmospheric temperature gradient near the tangent height. Since the mean air mass traversed by the sets of rays reaching an instrument is obtained by weighting over the FOV these results show that the weighting is a function of the temperature profile and changes in the temperature gradient must be considered when the mixing-ratio profile is obtained from actual data.

## Summary

The amount of an absorbing gas along the atmospheric paths traversed by solar rays can be obtained from the equivalent widths of weak absorption lines in solar spectra provided the models used to describe the geometry of the experiment and the structure of the atmosphere are known. The effects of systematic errors in these parameters on the retrieved mixing-ratio profiles of the absorber have been estimated. With the exception of the effects of atmospheric refraction and errors in the temperature profile these errors produce nearly identical effects on the retrieved profiles. These effects are equivalent to an error in the tangent heights of the rays producing the set of spectra which is independent of the height of the ray. The magnitudes of these effects agree with those estimated by making simplifying assumptions about the experiment design.

The existence of these errors can be detected by comparing the mixing-ratio of a gas whose vertical distribution in the atmosphere is known with that obtained by analyses of the equivalent widths of its lines in the spectra. However, because of the similarities of these effects it is not possible to determine, from these profile differences, either the number of parameters in Table 2 which are in error or the magnitudes of these errors unless additional information is supplied or different types of measurements are made. No discussion of the influence of several smearing effects present in the spectra on the derived mixing-ratios has been given although it has been pointed out that these can substantially reduce the vertical resolution.<sup>11</sup> Incorrectly modelled smearing effects may lead to systematic errors substantially larger than those in Table 2. In the remainder of this discussion the method of internal calibration is discussed. Although

itself subject to systematic errors these are expected to be small. This method does avoid many of the errors due to the incorrect modelling of smearing effects as well as many of the systematic errors discussed above.

#### Internal Calibration of Occultation Spectra

When the information about the atmospheric paths is obtained from external sources several errors affect the retrieved profiles in nearly identical ways. This occurs, in part, because the spectral information concerning the atmosphere, carried by a ray with a fixed tangent height and which originates outside the atmosphere, and is collected outside the atmosphere, is not influenced by the positions of either the source or the detector along the ray and hence by the particular sets of parameters which describe these positions. It has also been noted that the quality of the spectra is degraded by the finite FOV of the instrument, satellite motion,<sup>11</sup> atmospheric refraction, and temperature - and density - profile variations along the atmospheric path<sup>12</sup> and that it is unlikely that all of these effects can be satisfactorily modelled in the analysis.

Internal calibration removes many of these uncertainties but also introduces new ones. In this method, information about the atmospheric path is obtained from absorption lines in the spectra. Lines of  $\text{CO}_2$  are often measured because its vertical and latitudinal mixing-ratio is nearly constant and the parameters of many  $\text{CO}_2$  lines are accurately known. We consider, initially, the information obtained by measuring the equivalent width of a single weak  $\text{CO}_2$  line, with a temperature-independent line intensity, in a single spectrum. This allows one aspect of the path, such as the total amount of  $\text{CO}_2$ , to

be obtained. The additional information obtained by measuring the equivalent widths of several lines in different regions of the curve of growth, by measuring lines whose intensities are temperature dependent, or by measuring the shapes of lines is considered later.

If  $W_0$  and  $W_1$  are the equivalent widths, in a single spectrum, of weak lines of  $CO_2$  and a trace gas, respectively, and if the corresponding line intensities  $S_0$  and  $S_1$  are temperature independent, then, from Eq. (3), the amount of  $CO_2$  along the path

$$a_0 = W_0 / S_0, \quad (18)$$

and the amount of the other absorber

$$a_1 = W_1 / S_1. \quad (19)$$

If the  $CO_2$  mixing-ratio  $\rho_0$  is constant with height and along the path traversed then the total air mass traversed

$$A = W_0 / S_0 \rho_0, \quad (20)$$

and the mean mixing-ratio of the absorber along the ray path, relative to that of  $CO_2$

$$\rho_1 = a_1 / A. \quad (21)$$

These simple results are obtained because the incremental equivalent widths are additive.

In this approach both equivalent widths have been averaged in some (unknown) manner over the FOV of the instrument and they are weighted by the other factors discussed above which affect the quality of the data. If the spectra are obtained by a Fourier Transform Spectrometer information concerning both of the lines  $W_0$  and  $W_1$  is collected simultaneously. Provided the lines are both weak and neither of the mixing-ratios change rapidly over the FOV both of their equivalent widths are subjected to the same weighting processes which are then automatically ratioed out of the final results. Thus the values



for the total air mass traversed and the mean mixing-ratio of the unknown absorber given by Eqs. (19) and (21) do not contain the implicit uncertainties associated with the uncorrectable smearing effects of the external calibration methods.

Additional measurements or assumptions are still required to obtain the distribution of the unknown absorber with height. In the previous paper<sup>3</sup> this distribution was obtained from the measured equivalent widths  $W_1$  and the known geometry and the atmospheric structure. Thus the mixing-ratios could be determined either as a function of altitude or of pressure.

In the internal calibration method the geometry is inferred by comparing the  $W_0$  measurements with another set obtained from Eq. (20) and by assuming the atmospheric temperature, density, and  $CO_2$  profiles are known. The unknown mixing-ratio is then obtained as described previously.<sup>3</sup> These atmospheric paths will differ from the actual paths if these assumed profiles are incorrect. Thus errors in the mixing-ratio profile of the unknown absorber will occur which will depend on the nature of the systematic error and the method used to describe the profile. For example, an error of  $\Delta P_0$  (e.g. of one percent) in the reference pressure  $P_0$  does not affect the estimates of the total air mass traversed since air masses are derived from Eq. (20). However, from Eq. (11) it can cause a corresponding error  $\Delta h$  ( $\sim 0.1$  km) in the tangent heights of all rays and hence the entire mixing-ratio is displaced vertically by  $\Delta h$ .

The effects of other types of errors can be estimated in a similar fashion and they are listed in Table 3. With the exception of errors in the temperature profile these effects are independent of the tangent heights of the rays. If the values in Table 3 are

ORIGINAL PAGE IS  
OF POOR QUALITY

added in quadrature the total uncertainty is less than 1 km. This is less than the vertical resolution due to the smearing effects already discussed. It is also smaller than the vertical resolution of the trace gas profiles expected to be obtained from mid-infrared, occultation spectra obtained with state of the art Fourier transform spectrometers at balloon or satellite altitudes. If reasonable assumptions are made concerning the rate of data collection and the SNR this resolution is typically several kilometers. Thus internal calibration is appropriate for these measurements.

The internal calibration method does require the  $\text{CO}_2$  line intensities and its mixing-ratio. Although the spectrum of  $\text{CO}_2$  has been extensively investigated the wide range of intensities required to obtain accurate equivalent width information may require additional quantitative laboratory measurements of  $\text{CO}_2$  spectra. A careful evaluation of the global and temporal variations<sup>4</sup> in the atmospheric  $\text{CO}_2$  mixing-ratio is also needed. Mauersberger and Finstead<sup>13</sup> have summarized some of the information on atmospheric  $\text{CO}_2$  and have described some higher-than-expected  $\text{CO}_2$  mixing-ratios obtained above 25 km at night.

Some additional types of information which may improve the accuracy of the results is discussed below.

#### Relative Times of Data Collection

The rate of change  $dz_1/dt$  of the zenith angles of the incoming rays and the corresponding rate of change  $db/dt$  of the tangent height of rays reaching a satellite are nearly constant in a given occultation. Thus the scatter in the equivalent tangent heights

b<sub>1</sub> with time allows the consistency of the data to be estimated. Nearly constant systematic shifts between all of the values obtained by internal calibration of the spectra and those calculated from the orbital parameters may be due, for example, to timing errors. Differences at low tangent heights below 10 km may be caused by improperly corrected refraction effect and uncertainties in the CO<sub>2</sub> mixing-ratio or departures from LTE may produce differences between the observed and calculated curves for tangent heights above 70-80 km. However, good agreement can usually be expected for rays with tangent heights between about 20 and 50 km and these data can be used to improve the calibration of spectra which do not contain CO<sub>2</sub> lines suitable for calibration.

#### Measurements of Several Lines

The bands and lines of CO<sub>2</sub> have a wide range of intensities. Thus by measuring the equivalent widths of a number of lines in each spectrum the consistency of the measurements can be estimated and those lines which are too weak to be measured accurately or which lie outside the linear region, can be rejected. The effective SNR is also improved by measuring a number of lines.

Because of the very large variation in the air masses traversed by rays with tangent heights from 0 to above 50 km it is necessary to measure CO<sub>2</sub> lines with a corresponding range of temperature-independent intensities in order to maintain high precision. In general, this will require measurements of CO<sub>2</sub> lines, with small lower state energies, in bands with different intensities.

### Lines Not in the Linear Region

It has so far been assumed that the equivalent widths of the CO<sub>2</sub> calibration lines can be obtained from Eq. (1), which can be written as

$$W(z_1) = \sum_i \Delta W_{ij}.$$

If the CO<sub>2</sub> lines are not in the linear region of the curve of growth the incremental widths  $\Delta W_{ij}$  depend on the local atmospheric temperature and density and they are no longer additive. The weighting of such lines over the FOV and other smearing effects is different from that for weaker CO<sub>2</sub> lines or weak lines of trace gases.

In these cases one of the principal advantages of the internal calibration method, the ability to assume that the smearing effects are the same for all lines, is lost. It is therefore important to choose CO<sub>2</sub> calibration lines which are in or close to the linear region of the curve of growth.

### Measurements of Temperature Dependent Lines

Because the atmosphere is not isothermal the weighting of the equivalent widths of the lines over the FOV depends on the temperature dependence of the lines in addition to other effects previously considered. Since the strongest lines of most trace gases are not strongly temperature dependent CO<sub>2</sub> lines with a similar temperature dependence should be chosen for calibration. Discussions of the atmospheric information contained in temperature dependent CO<sub>2</sub> lines are given elsewhere.<sup>14,15</sup>

### Curve Fitting

Spectral curve-fitting is a powerful method of extracting information

if the models describing the spectrum are accurate.<sup>16,17</sup> Park<sup>11</sup> has shown that the effects of satellite motion during data collection and also other effects distort the occultation interferograms and consequently the spectra derived from them and that these smearing effects on the line shapes are difficult to model accurately. These methods are not explored in this paper. Shaffer and Shaw<sup>3</sup> have shown that more information on the vertical distribution of gases can be obtained by collecting as many spectra as possible during an occultation than by inferring the distribution from the profiles of the lines in a single spectrum. One of the principal effects of measuring equivalent widths is to smooth the noise in the data analyzed.

#### Conclusions

Internal calibration of satellite occultation spectra from measurements of the equivalent widths of weak, temperature-independent  $\text{CO}_2$  lines may be preferable to calibration based on error-prone external information. It is expected that internal calibration should allow the mean tangent heights of the rays to be estimated to about 1 km and the mixing ratios of trace gases to about five percent.

These uncertainties increase if the intensities of the lines used for calibration are temperature dependent and if the lines are not in the linear region of the curve of growth because the weighting of the absorber over the FOV and other smearing effects depend on the line parameters.

However, because of the large numbers and the wide range of intensities of  $\text{CO}_2$  lines appearing in the solar spectrum the accuracy of the internal calibration method can be maintained over wide height intervals.

Table 1. Quantities Affecting the Equivalent  
Widths of Weak Lines in Solar Spectra

Variable	Parameter
Line Intensity	Atmos. temperature
Atmos. density	height sea level pressure Atmos. temperature profile
geometrical path	observer altitude atmos. refraction latitude angle of arrival of ray

Table 2. Sources of Error and Their Effects  
on Retrieved Mixing Ratio Profiles

ORIGINAL PAGE IS  
OF POOR QUALITY

Quantity in Error	Mixing Ratio Error, Dependence on Height	Change Required for 1% Error in Mixing Ratio
Refraction	only important below 25 km	
Reference Pressure	independent of height	$\Delta P_0 = 10 \text{ mb}$
Temperature Profile	increases with height	
Satellite Height	independent of height	$\Delta h = 80 \text{ m}$
Latitude	" " "	
Radius of Earth	" " "	1 km (at 45°)
Angle of Incoming Rays	" " "	0.002°
Time of obs.	" " "	0.03 secs
Position in orbit	" " "	0.25 km

Table 3. Dependence of the Errors in the Tangent Heights of Rays  
Made by Using Internal Calibration Methods on  
Systematic Errors in the Assumed Parameters Values

Parameter	Systematic Fractional Errors (%)	Corresponding Change in Tangent Height of Rays
Sea level pressure	1	0.1 km
Temp Profile	1 (3K)	<u>&lt;</u> 0.5 km
CO <sub>2</sub> mixing ratio	1	0.1 km
Line intensity	1	0.1 km
Equivalent width	1	0.1 km



- Fig. 1 Occultation Geometry. For a mean earth radius  $R = 6360$  km and a satellite height  $a = 500$  km the distance  $L$  is about 2500 km, the angle  $\Theta$  is about  $21^\circ$  and the zenith angle  $z$  is about  $111^\circ$ .
- Fig. 2 The dependence of the air mass traversed by rays with tangent heights of approximately 3, 12, and 48 km on the thickness of the atmospheric layers used in the calculation. The fractional change in air mass with respect to that calculated for 25 m thick layers is shown.
- Fig. 3 The dependence of the fractional air mass error along the rays, due to the neglect of atmospheric refraction, on the tangent height of the rays for the case of an observer at 500 km.
- Fig. 4 The height dependence of the fractional errors in the mixing-ratio profile caused by the neglect of atmospheric refraction in the retrieval.
- Fig. 5 The height dependence of the fractional errors in the mixing ratio profile caused by five percent errors in sea level pressure.
- Fig. 6 The height dependence of the fractional errors in the retrieved mixing-ratio profile caused by assuming  $\pm 5$  K changes at all heights in the U. S. Standard Atmosphere temperature profile.
- Fig. 7 The height dependence of the fractional errors in the retrieved mixing-ratio profile caused by errors of  $\pm 1$  km in the satellite height.
- Fig. 8 The height dependence of the fractional errors in the retrieved mixing-ratio profile caused by errors of  $\pm 0.01^\circ$  in the angles of the incoming rays.

Fig. 9 Fractional rate of change of air mass ( $\text{sec}^{-1}$ ) for an observer at 500 km

a) U.S. Standard Atmosphere b) atmosphere with a temperature gradient of 1 K/km. The tangent heights of the rays decrease from 90 to 0 km.

1. C. B. Farmer, NASA Upper Atmosphere Research Program Summaries (1982).
2. C. B. Farmer, D. F. Raper, B. D. Robbins, R. A. Toth, and C. Muller, *J. Geophys. Res.* 85, 1621 (1980).
3. W. A. Shaffex, Ph.D. diss. Ohio State Univ. (1983); W. A. Shaffer and J. H. Shaw, *Appl. Opt.* 22, 2977 (1983).
4. "The Stratosphere 1981 Theory and Measurements", WMO Global Ozone Research and Monitoring Project Report No. 11 (1982).
5. D. E. Snider, *J. Atmos. Sci.* 32, 2178 (1975).
6. D. E. Snider and A. Goldman, BRL Report 1790, Aberdeen Proving Ground, Md. 21005 (1975).
7. U. S. Standard Atmosphere 1976, U. S. Govt. Print Office, Washington, D. C. (1976).
8. A. J. Kantor, "Variability of Atmospheric Density in the Middle Atmosphere," AFGL-TR-83-0079, AFGL, Hanscom AFB Mass 01781 (1983).
9. O. K. Garriott, *JOSA* 69, 1064 (1972).
10. J. M. Russell, III, *Pure and Appl. Geophys.* 118, 616 (1980).
11. J. H. Park, *Appl. Opt.* 21, 1356 (1982).
12. D. A. Roewe, J. C. Gille, and P. L. Bailey, *Appl. Opt.* 21, 3775 (1982).
13. K. Mauersberger and R. Finstead, *Geophys. Res. Lett.* 7, 873 (1980).
14. R. A. Toth, *Appl. Opt.* 16, 2661 (1977).
15. C. F. Rinsland, A. Goldman, F. J. Murcray, D. G. Murcray, M. A. H. Smith, R. K. Seals, Jr., J. C. Larsen and P. L. Rinsland, *JQSRT* 30, 237 (1983).
16. Y. S. Chang, J. H. Shaw, J. G. Calvert, and W. M. Ueselman, *JQSRT* 19, 599 (1978).
17. E. Nigle and J. H. Shaw, *Appl. Spectros.* 33, 569 (1979).

ORIGINAL PAGE IS  
OF POOR QUALITY

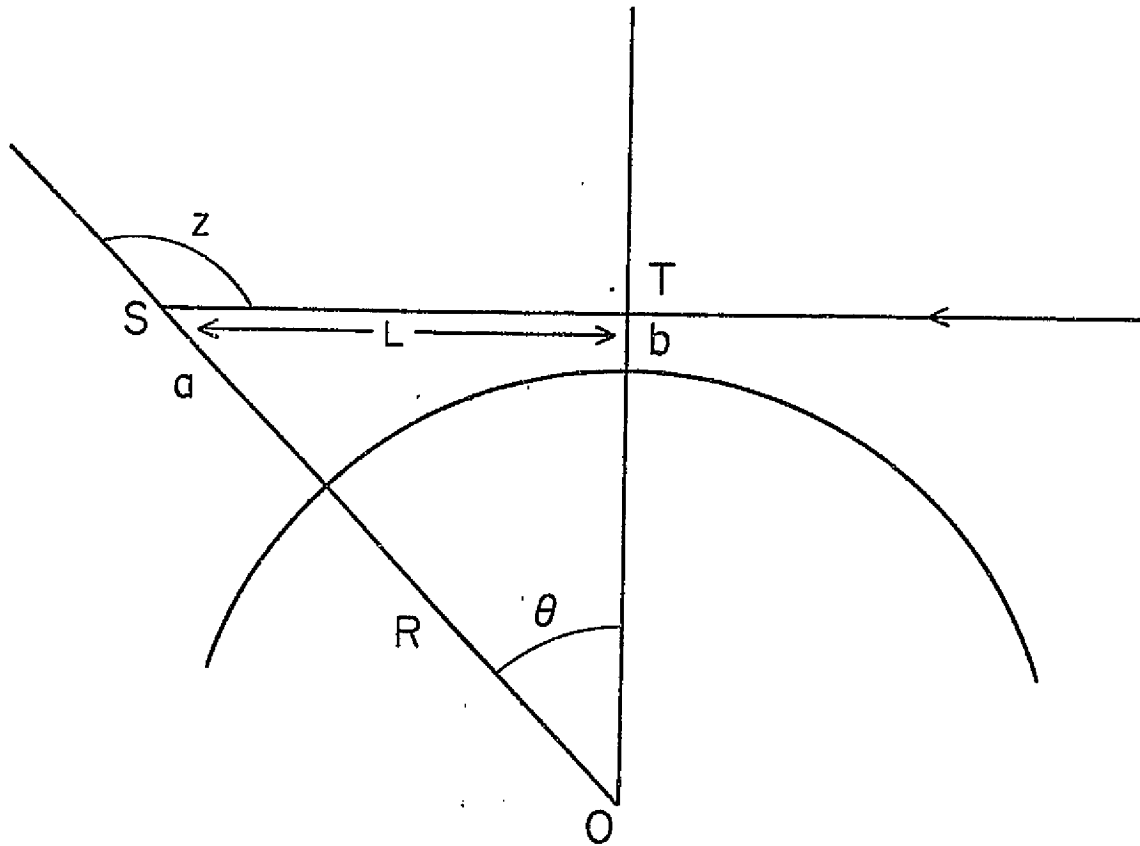


Fig 1

ORIGINAL PAGE IS  
OF POOR QUALITY

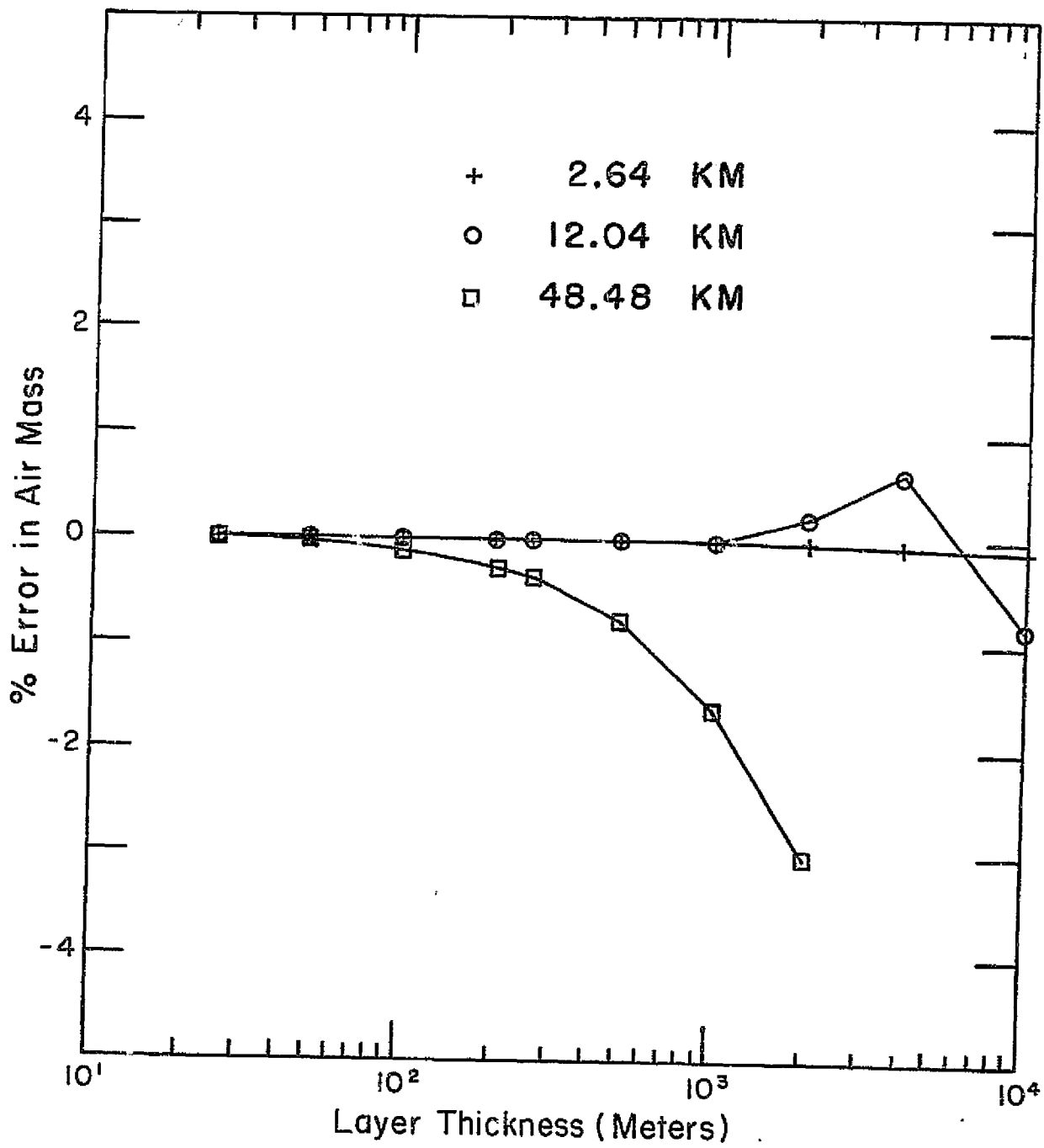


Fig. 2

ORIGINAL PAGE IS  
OF POOR QUALITY

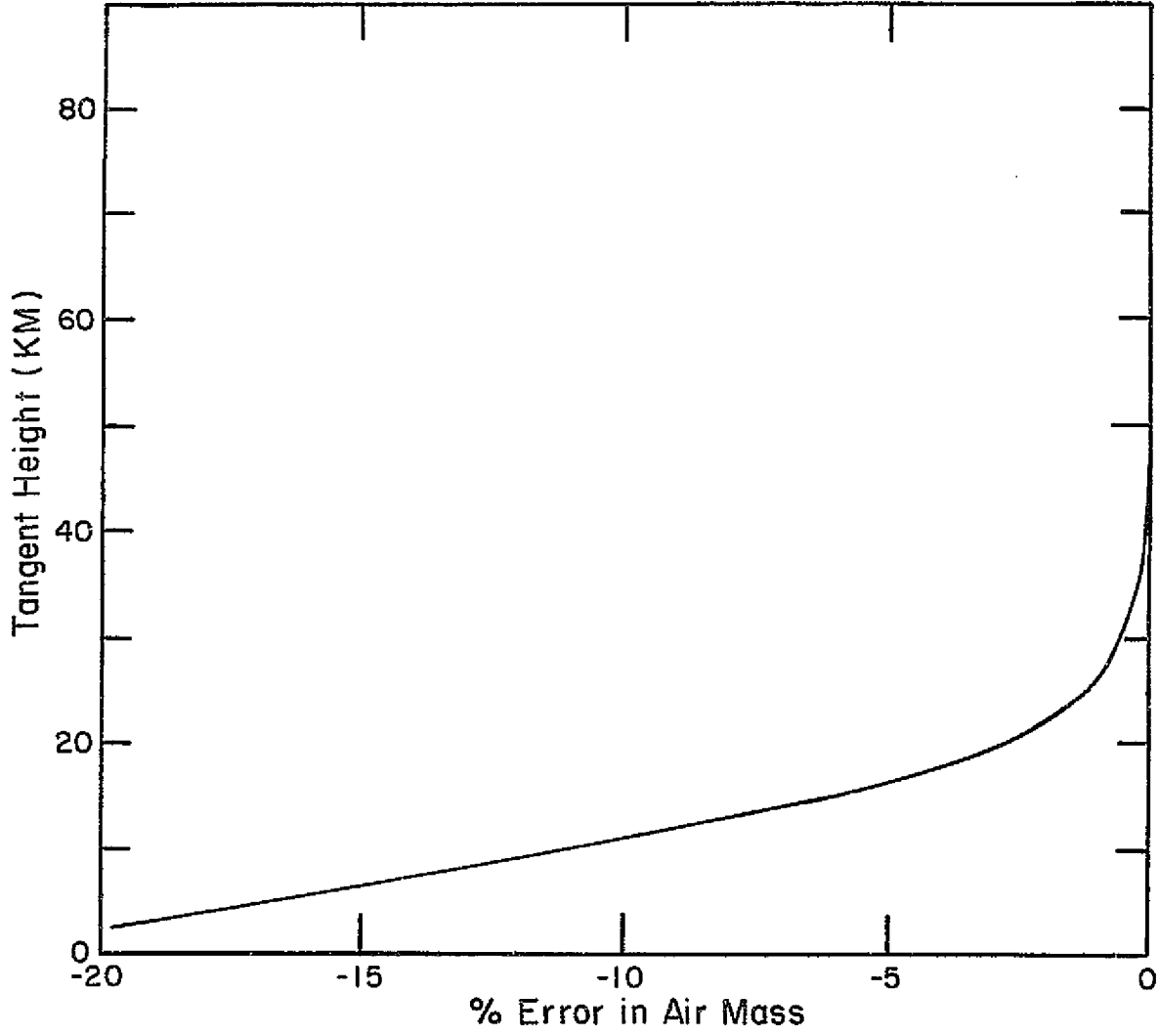


Fig. 3

ORIGINAL PAGE IS  
OF POOR QUALITY

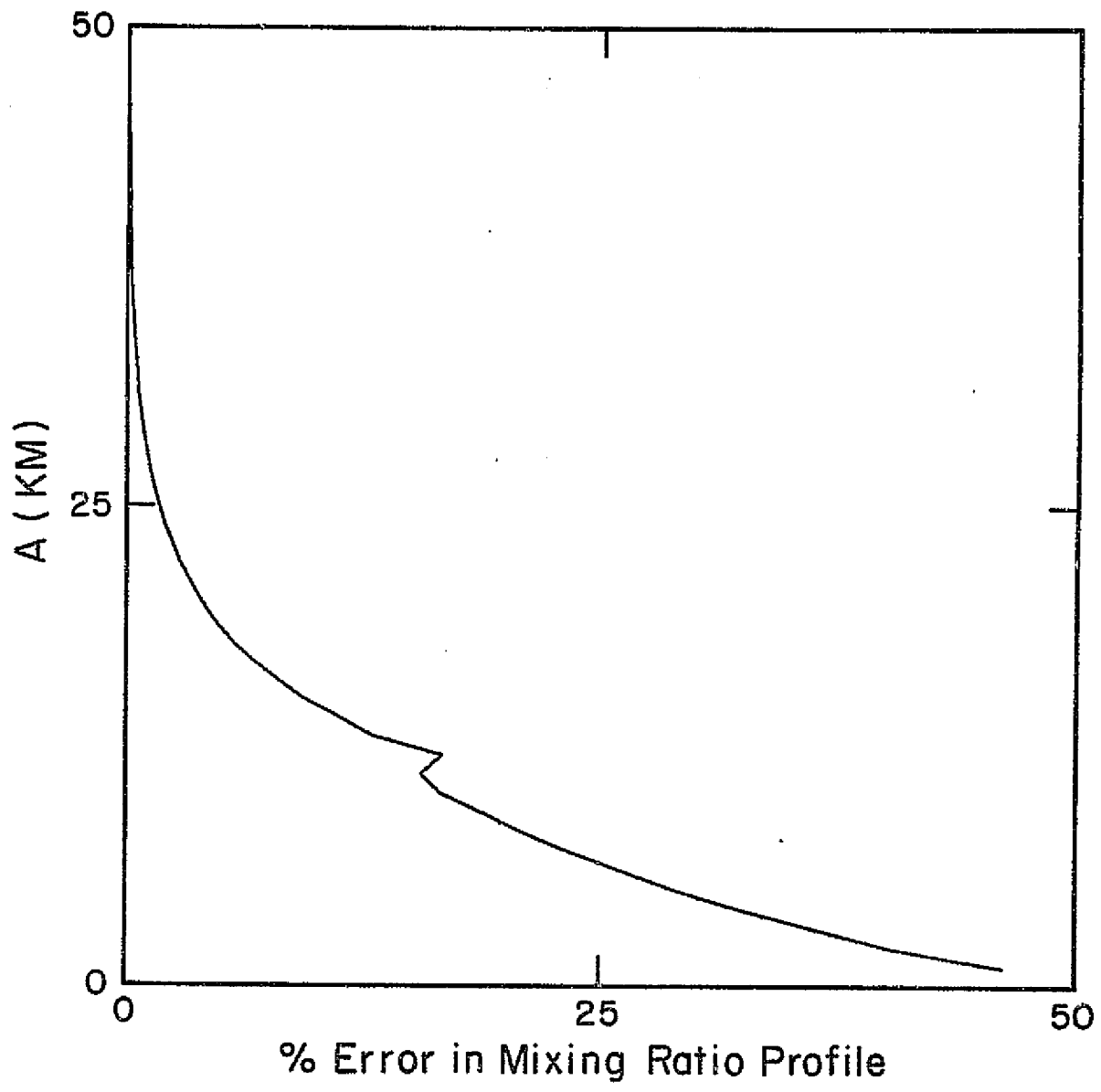


Fig. 4

ORIGINAL PAGE IS  
OF POOR QUALITY

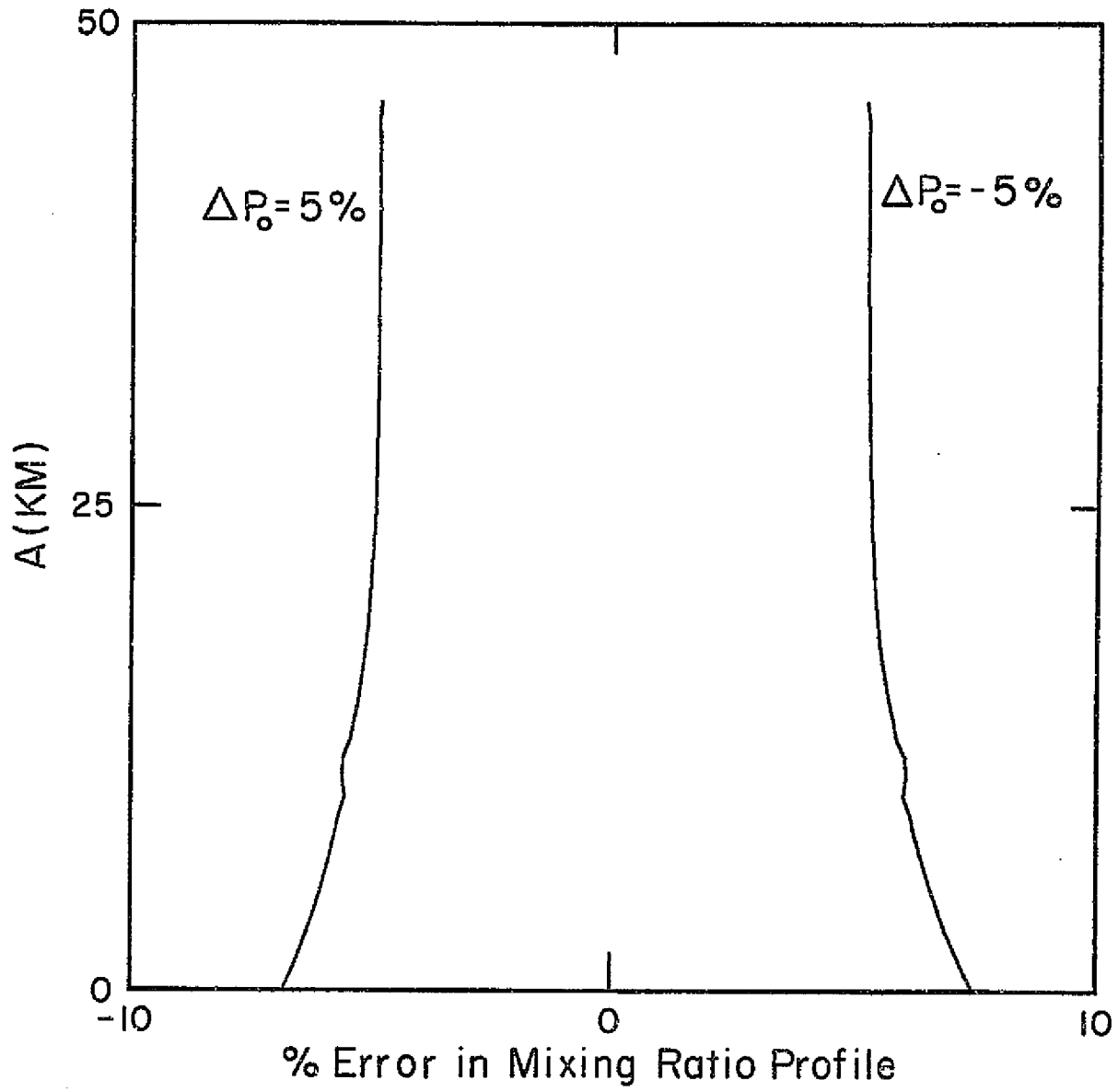


Fig: 5



ORIGINAL PAGE IS  
OF POOR QUALITY

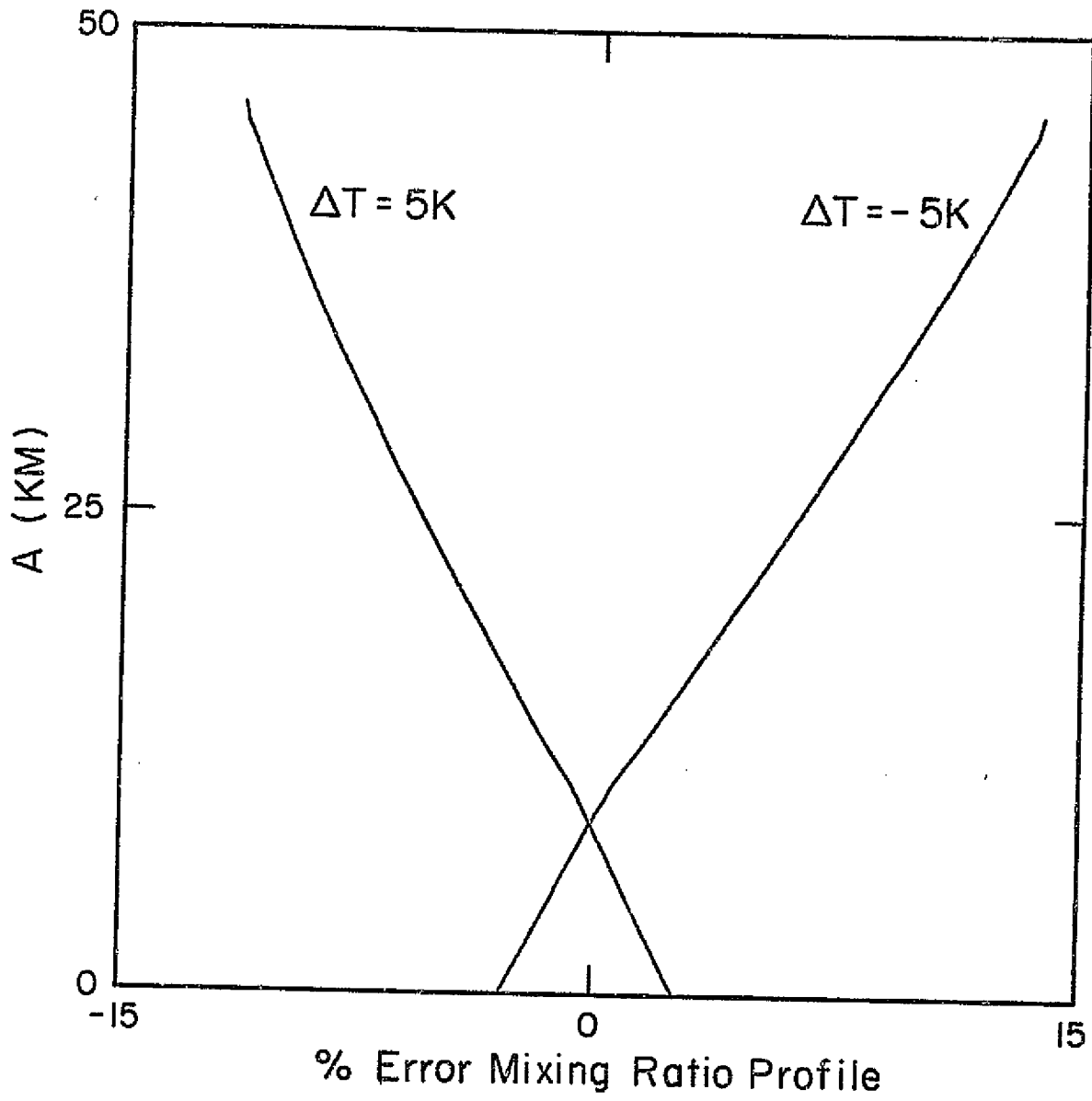


Fig. 6

ORIGINAL PAGE IS  
OF POOR QUALITY

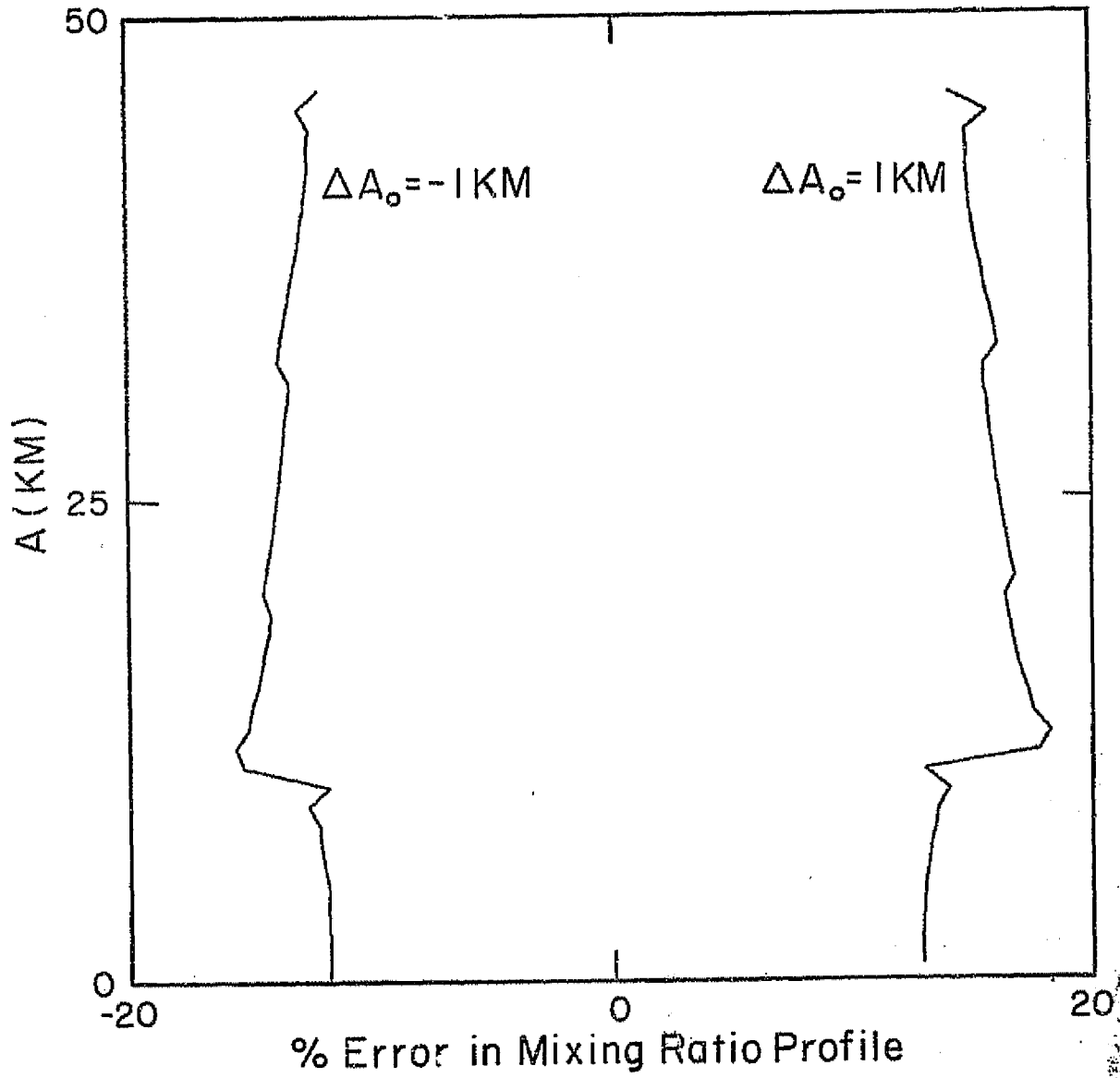


Fig. 7

ORIGINAL PAGE IS  
OF POOR QUALITY

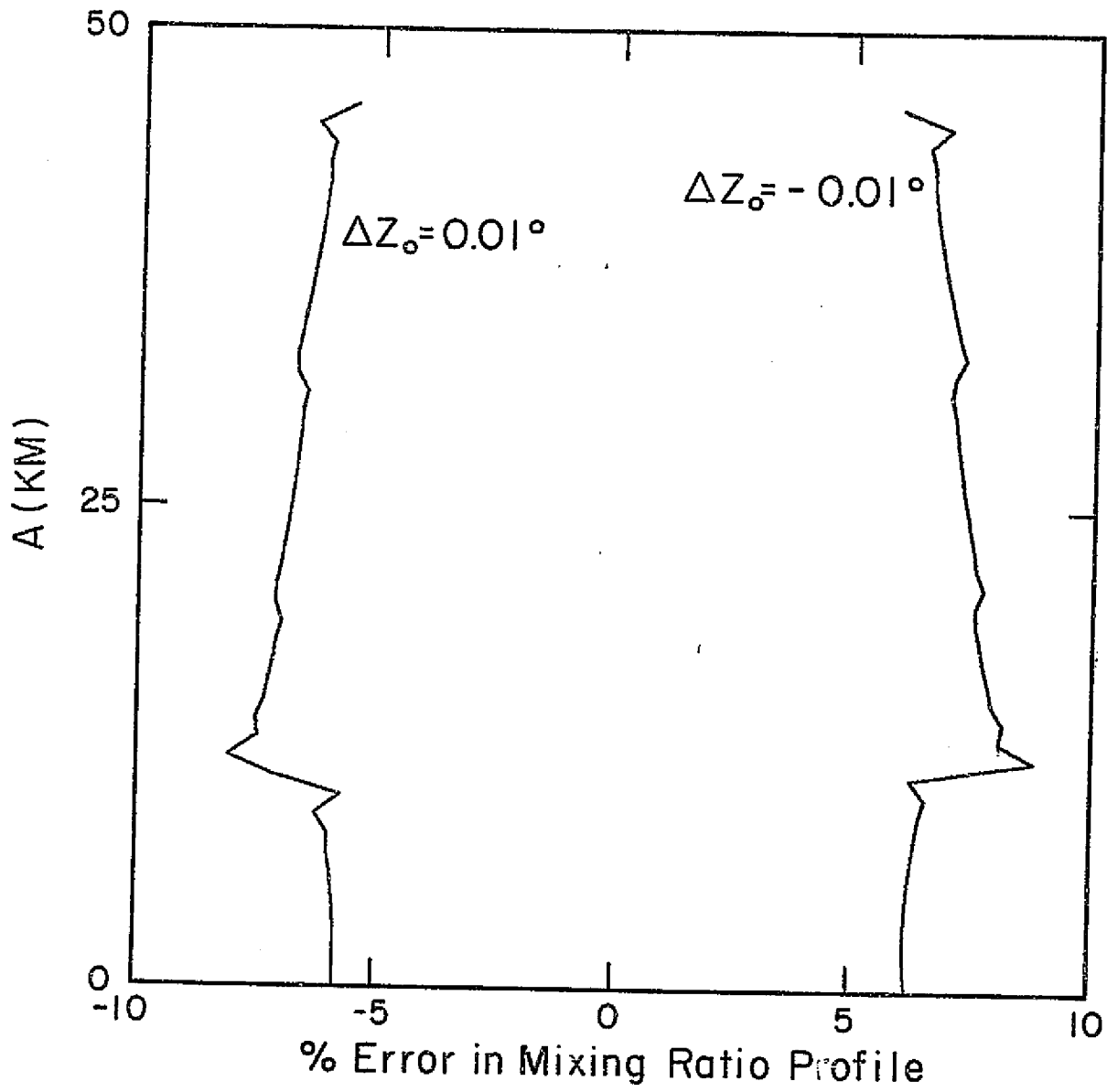


Fig. 8

ORIGINAL PAGE IS  
OF POOR QUALITY

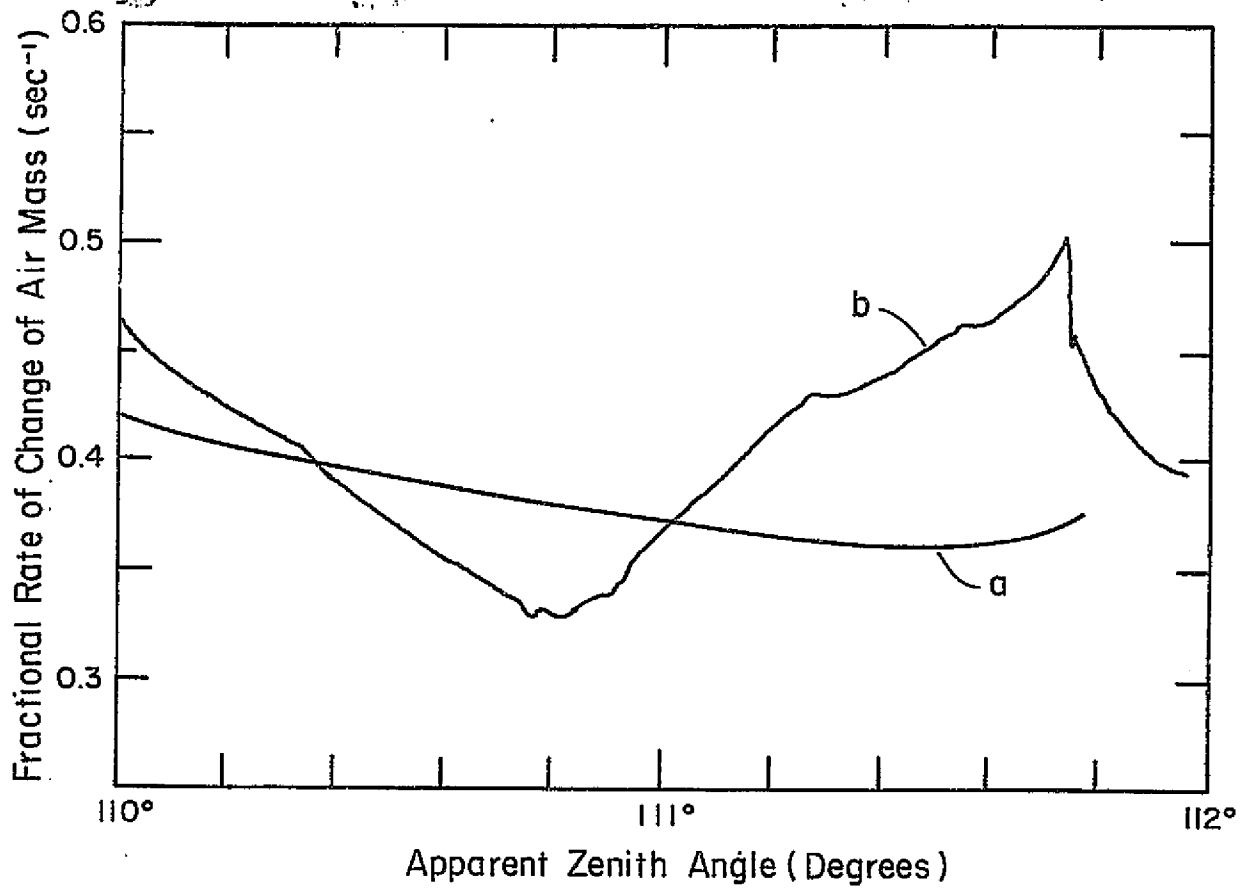


Fig. 9